Weierstraß-Institut für Angewandte Analysis und Stochastik

Leibniz-Institut im Forschungsverbund Berlin e. V.

Preprint ISSN 2198-5855

Coherence properties of Kerr frequency combs under noisy injection and optical feedback

Varvara lachkula¹, Daria A. Dolinina², Andrei G. Vladimirov³, Guillaume Huyet¹

submitted: October 29, 2025

Université Côte d'Azur, CNRS
 Institut de Physique de Nice (INPHYNI)

 06200 Nice
 France

E-Mail: varvara.iachkula@univ-cotedazur.fr guillaume.huyet@univ-cotedazur.fr

- Ferdinand-Braun-Institut (FBH)
 Gustav-Kirchhoff-Str. 4
 12489 Berlin
 Germany
 - E-Mail: daria.dolinina@fbh-berlin.de
- Weierstrass Institute Anton-Wilhelm-Amo-Straße 39 10117 Berlin Germany

E-Mail: andrei.vladimirov@wias-berlin.de

No. 3225 Berlin 2025



2020 Mathematics Subject Classification. 78A60 35B32 35C08 35Q60.

2010 Physics and Astronomy Classification Scheme. 42.65.-k 42.65.Sf 42.65.Pc 42.65.Tg 05.45.-a 42.60.Mi.

Key words and phrases. Kerr frequency combs, optical microresonators, Lugiato-Lefever equation, phase noise, timing jitter, delayed optical feedback.

This work was supported by the HYBRIDCOMB project, funded by the ANR and the DFG (No. 491234846). The part of this work contributed by D.A. Dolinina was carried out while she was affiliated with WIAS.

Edited by
Weierstraß-Institut für Angewandte Analysis und Stochastik (WIAS)
Leibniz-Institut im Forschungsverbund Berlin e. V.
Anton-Wilhelm-Amo-Straße 39
10117 Berlin
Germany

Fax: +49 30 20372-303

E-Mail: preprint@wias-berlin.de
World Wide Web: http://www.wias-berlin.de/

Coherence properties of Kerr frequency combs under noisy injection and optical feedback

Varvara lachkula, Daria A. Dolinina, Andrei G. Vladimirov, Guillaume Huyet

Abstract

Kerr frequency combs in high-Q optical microresonators hold great promise for precision metrology, high-speed communications, and low-noise photonics. Understanding their coherence properties is essential for realizing compact, energy-efficient, and low-noise light sources. The interplay between pulsed injection, intrinsic and external noise, and optical feedback plays a central role in achieving highly coherent microcombs. Here, we study the coherence dynamics of Kerr frequency combs under continuous-wave (CW) and pulsed pumping within the framework of the Lugiato-Lefever equation. Using asymptotic analysis, we quantify the phase noise and timing jitter induced by pump source fluctuations and thermal noise. Numerical simulations further reveal comb degradation due to CW pump noise, while the inclusion of optical feedback restores the comb and narrows the linewidth through a mechanism analogous to that of external-cavity lasers.

1 Introduction

Solitons in nonlinear optical systems play a central role in modern photonics, offering exceptional stability and enabling transformative applications in high-precision frequency comb generation, ultrafast optics, and optical communications. Kerr microcavities, described by the Lugiato-Lefever Equation (LLE) [17, 18], provide a powerful platform to study soliton dynamics. The LLE captures the essential physical ingredients of these systems, including dispersion, Kerr nonlinearity, cavity losses, and external driving, making it a cornerstone model for understanding frequency comb formation.

A particularly successful approach for generating compact optical frequency combs in microcavities relies on continuous-wave (CW) pumping. In this configuration, spatial solitons spontaneously form and circulate periodically in the cavity, creating a stable pulse train in the time domain and a coherent frequency comb in the spectral domain. However, these solitons are sustained on top of a CW background, leading to inefficient energy transfer from the pump source.

To improve efficiency, the CW pump can be replaced by a mode-locked laser with a repetition rate synchronized to the round-trip time of the cavity. In this regime, broad optical pulses from the mode-locked laser coherently excite solitons in the microcavity, enabling broadband comb generation. Using the LLE framework, it has been shown that cavity solitons can synchronize (or lock) to the external pulse train, even when the repetition rate of the pump does not exactly match the cavity's free spectral range [10, 11, 9, 5, 24, 4, 3].

Despite their robustness, solitons are vulnerable to various sources of noise, which degrade comb stability and coherence. Stochastic perturbations, such as pump laser phase noise and thermore-fractive fluctuations within the microresonator, introduce amplitude, phase, and timing jitter. These effects broaden the comb linewidth [12, 23, 14, 7], degrade temporal coherence, and disrupt synchronization—particularly near bifurcation points where the soliton state becomes more sensitive to

perturbations [16, 19, 6]. In this context, understanding the impact of noise is critical for advancing soliton-based technologies in metrology, sensing, and communication systems.

Among the different noise sources, fluctuations in the injected pump beam play a dominant role. Phase noise, arising from temporal decoherence of the laser source, increases the effective linewidth of the pump and destabilizes the soliton. Timing jitter in pulsed pumping configurations adds further instability by perturbing the synchronization between the driving field and the circulating soliton. Prior work has demonstrated that all-optical synchronization can reduce the influence of internal noise by locking the microcomb to a reference laser [21], but this also increases susceptibility to external noise.

Injection locking studies have shown how phase noise from the pump can be transferred to the comb [26], while noise amplification mechanisms have been investigated for low-phase-noise THz generation [13]. Theoretical efforts have also explored how amplitude and phase noise influence the comb repetition rate [20], and experimental studies have highlighted the effect of timing jitter on synchronously pumped microcavity solitons [2, 1, 5].

This paper investigates analytically and numerically the combined impact of phase noise and injection pulse timing jitter on soliton dynamics in synchronously pumped Kerr microcavities, using the LLE as the governing model. We perform an asymptotic analysis of the impact of external injection noise and intracavity thermal noise on soliton phase noise and timing jitter.

We show that the soliton destabilization induced by these noise sources can be understood in terms of both the noise strength and the system's proximity to bifurcation points. Furthermore, we demonstrate that even when the noise level is sufficient to destroy the soliton state, recovery is achievable through the application of coherent feedback to the microcavity. By analyzing the mechanisms through which noise disrupts soliton dynamics, this work identifies fundamental limitations and proposes strategies to enhance soliton robustness in noisy environments thereby supporting the development of reliable and noise-resilient frequency comb technologies.

We consider the dynamics of the intracavity field A(x,t) in a synchronously pumped Kerr microcavity, described by a stochastic version of the LLE. After rescaling and setting the dispersion coefficient to one, the governing equation becomes:

$$\frac{\partial A}{\partial t} = -A - i[\theta + \sigma(t)]A + i\frac{\partial^2 A}{\partial x^2} + [v + \beta(t)]\frac{\partial A}{\partial x} + A_{\rm in}[x + \xi(t)]e^{i\phi(t)}, \quad (1)$$

where A(x,t) is the slowly varying envelope of the intracavity field satisfying periodic boundary condition A(x,t)=A(x+L,t), where t (x) is the slow (fast) time, and L is the cavity round trip time. The term -A accounts for cavity losses, $-i[\theta+\sigma(t)]A$ models cavity detuning θ , with an additional stochastic fluctuation $\sigma(t)$ representing detuning noise, $i\frac{\partial^2 A}{\partial x^2}$ captures group velocity dispersion in the cavity, $[v+\beta(t)]\frac{\partial A}{\partial x}$ includes a constant drift velocity v due to the difference between the pump and microcavity repetition rates, and a time-dependent stochastic drift $\beta(t)$ accounting for the cavity thermal fluctuations, $A_{\rm in}[x+\xi(t)]\cdot e^{i\phi(t)}$ is the injected pulse, subject to timing jitter $\xi(t)$ and phase noise $\phi(t)$.

The noise processes $\xi(t)$ and $\phi(t)$ are Brownian motions, described by following Langevin equations:

$$d\phi = \sqrt{2D_{\phi}}\eta_{\phi}dt,\tag{2}$$

$$d\xi = \sqrt{2D_{\xi}}\eta_{\xi}dt,\tag{3}$$

where each $\eta_i(t)$ describes white noise process.

The thermal fluctuations of the cavity can be described by an Ornstein-Uhlenbeck (OU) process:

$$dT = -\kappa (T - T_0)dt + \sqrt{2D}\eta_T dt, \tag{4}$$

where κ is the temperature relaxation time, T_0 is the mean temperature of the cavity and $\eta_T(t)$ is a white noise process. Assuming that the refractive index depends linearly with the temperature, both $\sigma(t)$ and $\beta(t)$ are also described by OU processes. In the limit of short temperature relaxation times, both $\sigma(t)$ and $\beta(t)$ become white-noise processes.

2 Asymptotic analysis

Let us assume that the constant drift velocity, detuning noise, stochastic drift, and the phase and timing jitter diffusion coefficients are small, $v=\mathcal{O}(\varepsilon^2)$, $\beta(t)=\varepsilon\Upsilon(t)$, $\sigma(t)=\varepsilon\Sigma(t)$, and $D_{\phi,\xi}=\varepsilon^2 d_{\phi,\xi}$, where $\varepsilon\ll 1$. Furthermore, let the injection pulse be unchirped and in the absence of noise soliton is located at $x=x_0$ near the top of the injection pulse at x=0. If the injection pulse width is much broader than the microcavity soliton width, in the vicinity of the soliton core x=0, the injection pulse can be approximated by a parabolic function $A_{in}=\eta_0-\varepsilon\eta_2(x+\xi)^2/2+\mathcal{O}(\varepsilon^2)$ around the core.

In the unperturbed case ($\varepsilon=0$), Eq. (1) is transformed into the classical LLE with zero drift parameter, zero detuning noise, and CW injection $\eta_0 \exp(i\phi)$; Eqs. (2) and (3) become $\partial_t \phi=0$ and $\partial_t \xi=0$. Furthermore, Eq. (3) decouples from the rest of the system. Using the fact that in the unperturbed system $\phi=\phi_0$ and $\xi=\xi_0$ are constant we assume without the loss of generality that $\xi_0=\phi_0=0$. Then Eq. (1) is transformed into the standard LLE with the CW injection term η_0 . Let $A(x,t)=a_0(x)$ is the cavity soliton solution of this equation. The translational and phase symmetries of the unperturbed system (1 and 2) with $\varepsilon=0$ and $\sigma=\beta=0$, $\xi\to\xi+{\rm const}$ and $\phi\to\phi+{\rm const}$, imply the existence of two neutral modes of the operator \mathcal{L}_0 , obtained by linearizing this system around the soliton solution $a_0(x)$.

$$\mathbf{\Psi} = \begin{pmatrix} \partial_x \operatorname{Re} a_0 \\ \partial_x \operatorname{Im} a_0 \\ 0 \end{pmatrix}, \quad \mathbf{\Phi} = \begin{pmatrix} -\operatorname{Im} a_0 \\ \operatorname{Re} a_0 \\ 1 \end{pmatrix}$$

respectively. The corresponding translational and phase neutral modes of the adjoint linear operator \mathcal{L}_0^\dagger are:

$$\Psi^{\dagger} = \begin{pmatrix} \operatorname{Re} \psi^{\dagger *} & \operatorname{Im} \psi^{\dagger *} & 0 \end{pmatrix}, \quad \Phi^{\dagger} = \begin{pmatrix} 0 & 0 & 1 \end{pmatrix},$$

where the function $\psi(x)^\dagger$ is the translational neutral mode of the adjoint linear operator associated with the LLE having CW injection η_0 , which can be calculated numerically, and the superscript "*"denotes complex conjugation. The neutral modes satisfy the biorthogonality conditions $<\Psi\cdot\Psi^\dagger>=X_0^{-1}\int_0^L(\operatorname{Re}\psi^{\dagger*}\partial_x\operatorname{Re}a_0+\operatorname{Im}\psi^{\dagger*}\partial_x\operatorname{Im}a_0)dx=1$, and $<\Phi\cdot\Phi^\dagger>=L^{-1}\int_0^Ldx=1$, $<\Psi\cdot\Phi^\dagger>=<\Phi\cdot\Psi^\dagger>=0$.

Let us look for the solution of Eqs.(1-2) in the form:

$$A(x,t) = a_0(y) + \varepsilon a_1(t,x) + \mathcal{O}(\varepsilon^2),$$

$$\phi = \phi(\tau) + \varepsilon \phi_1(t) + \mathcal{O}(\varepsilon^2),$$

where $y=x-x_0-\zeta(\tau)$ and $\tau=\varepsilon t$. The shift x_0 of the soliton intensity peak relative to the maximum of the injection pulse in the absence of noise arises from the drift parameter v in Eq. (1). Since $v=\mathcal{O}(\varepsilon^2)$, it follows that $x_0=\mathcal{O}(\varepsilon^2)$, implying that neither v nor x_0 influences the subsequent analysis, which is carried out up to first-order terms in ε . Substituting this expression into model equations and collecting zero order terms in small parameter ε we get the unperturbed LLE which is satisfied automatically. Collecting the first order terms gives:

$$\mathcal{L}_0 \mathbf{V}_1 = \mathbf{\Psi}(y) \partial_\tau \zeta - \mathbf{\Phi}(y) \partial_\tau \phi + \mathbf{P}_1, \tag{5}$$

where
$$\mathbf{V}_1 = (\operatorname{Re} a_1, \operatorname{Im} a_1, \phi_1)^{\mathrm{T}}$$
 and $\mathbf{P}_1 = \Upsilon \Psi + \sqrt{2d_{\phi}} W_{\phi} \Phi + \begin{pmatrix} -\eta_2 (y + \zeta + \xi)^2 / 2 + \sigma & \operatorname{Im} a_0 \\ -\sigma & \operatorname{Re} a_0 \\ 0 \end{pmatrix}$

The solvability conditions of the first order equation (5) together with the symmetry considerations yield soliton phase drift equation:

$$d\phi = \left\langle \Phi^{\dagger} \cdot P_1 \right\rangle d\tau = \sqrt{2d_{\phi}} W_{\phi} d\tau, \tag{6}$$

and soliton noisy drift equation determining the soliton timing jitter:

$$d\zeta = -\left\langle \Psi^{\dagger} \cdot P_{1} \right\rangle d\tau = -\Gamma \zeta d\tau - \Upsilon d\tau - \Gamma \xi d\tau, \tag{7}$$

where the restoring constant

$$\Gamma = -(\eta_2/L) \int_0^L \operatorname{Re} \psi^{\dagger *}(y) y dy > 0$$

is determined by the overlap between the adjoint translation mode Ψ^\dagger and the pump profile. It follows from these asymptotic equations that in the leading order in ε the phase drift equation depends solely on the injection pulse phase noise and is unaffected by the detuning noise term σ . In contrast, the asymptotic equation (7) corresponds to an Ornstein–Uhlenbeck process that includes both drift and injection noise terms on the right-hand side. From this equation, one sees that in the limit of continuous-wave (CW) injection, where $\eta_2=0$, the injection noise term vanishes, and Eq. (7) reduces to an equation describing a Wiener process. Finally, using the relation $D_\xi=\varepsilon d_\xi$, we can rewrite Eq. (3) as:

$$d\xi = \sqrt{2d_{\xi}}W_{\xi}d\tau. \tag{8}$$

Equations (6) and (7) thus show that the phase noise of the injecting laser is directly transferred to the soliton phase noise in a straightforward manner. However, because the injection pulses are very broad, the timing jitter transmitted from the injection to the soliton is considerably suppressed due to the presence of the multiplier Γ in the last term of Eq. (7). In the limiting case of CW injection, the soliton jitter is entirely determined by the drift noise term β .

3 Microcavity with pulsed injection

In our numerical simulations, we compute the power spectra of both the intracavity electric field and its intensity. These quantities correspond, respectively, to the optical and radio-frequency (RF) spectra measured in experiments. It is well established that the linewidth of peaks in the RF spectrum provides direct access to the timing jitter of the pulse train, while the optical phase noise is directly linked to the linewidth of the individual comb teeth in the optical spectrum. This relationship can be illustrated by considering the idealized case of mode-locked pulses with repetition period T_r , phase noise $\Delta\phi(m)$ and timing jitter $\Delta t(m)$, both defined with Gaussian white noise:

$$A(t) = a_0 e^{i\phi_0(t)} + \sum_{m=-\infty}^{\infty} p(t - mT_r - \Delta t(m)) e^{i\omega_0(t - mT_r) - i\Delta\phi(m)},$$
(9)

where α_0 is the uniform background of the pulses defined by $\alpha(t)$, and ω_0 is the carrier frequency. The corresponding optical spectrum for pulse train consists of a set of Lorentzian lines [8] with frequencies

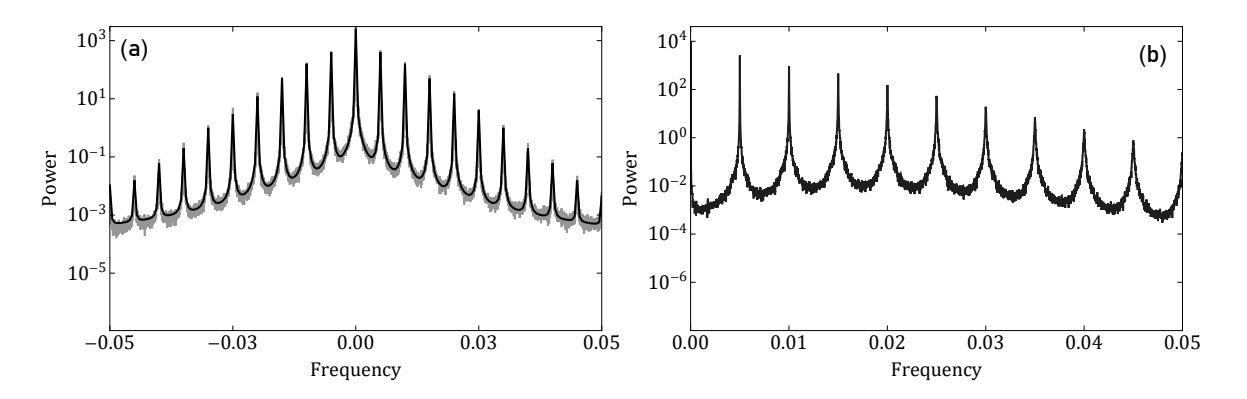


Figure 1: Optical (a) and RF (b) spectra obtained under pulsed injection with jitter and phase noise (black curve (a) - fitted Lorentzian lines).

 ω_n and linewidths $\Delta\omega_n$. It can be expressed as:

$$S(\omega) \sim |\alpha_0|^2 \frac{2\Delta\omega_0}{(\omega - \omega_n)^2 + \Delta\omega_0^2} + |\hat{a}(\omega - \omega_0)^2| \times \sum_{n = -\infty}^{\infty} \frac{2\Delta\omega_n}{(\omega - \omega_n)^2 + \Delta\omega_n^2}, \tag{10}$$

where $\Delta\omega_n$, with respect to phase $(\Delta\omega_{\phi})$ and timing jitter $(\Delta\omega_t)$ diffusion rates, is:

$$\Delta\omega_n = \Delta\omega_\phi + (\omega - \omega_0)^2 \tau^2 \Delta\omega_t,\tag{11}$$

Moving to the RF domain, the RF spectrum exhibits broadening due to timing jitter, with peaks centered at $m\omega_r=\frac{2m\pi}{T_r}$ harmonics with linewidths $\Delta\omega_{RF,m}$. The RF spectrum can be written as:

$$S_{RF}(\omega) \sim |\hat{a}(\omega - \omega_0)^2| \times \sum_{m=-\infty}^{\infty} \frac{2\Delta\omega_{RF,m}}{(\omega - m\omega_r)^2 + \Delta\omega_{RF,m}^2},$$
 (12)

where $\Delta\omega_{RF}$ is given by:

$$\Delta\omega_{RF,n} = (2\pi n\tau/Tr)^2 \Delta\omega_t,\tag{13}$$

Considering both (11) and (13) it is possible to relate linewidth values $\Delta\omega_n$ and $\Delta\omega_{RF,m}$ via:

$$\Delta\omega_n = \Delta\omega_0 + \Delta\omega_{RF,1}(n - n_0)^2,\tag{14}$$

From Eq. (14), it is evident that the system shows a parabolic dependence of the linewidth on the harmonic number, which directly results from the presence of timing jitter. To simulate the LLE with pulsed injection we employ the general form of Eq. (1), where the injection term A_{in} is defined as:

$$A_{in} = A_0 e^{\frac{-(x-\xi(t)}{2w^2}} e^{i\phi(t)},\tag{15}$$

By modeling Eq. (1) with an injection term A_{in} from Eq. (15), we obtained the corresponding optical and RF spectra (Fig. 1). Notably, the linewidth of each comb tooth increases with harmonic order as a result of a timing jitter. Based on these results, we further analyze the dependence of the linewidth. Following the approach of Haus and Mecozzi, and taking into account phase dynamics, we define the linewidth $\Delta \nu$ as:

$$\Delta \nu = \frac{D_{\phi}}{\pi},$$

The graphical representation of the linewidth dependence on the harmonic number (Fig. 2) clearly follows the quadratic trend observed in mode-locked lasers. This allows us to quantify timing jitter in high-repetition rate frequency combs and indicates that LLE exhibits behavior similar to that of a mode-locked laser in the presence of timing jitter.

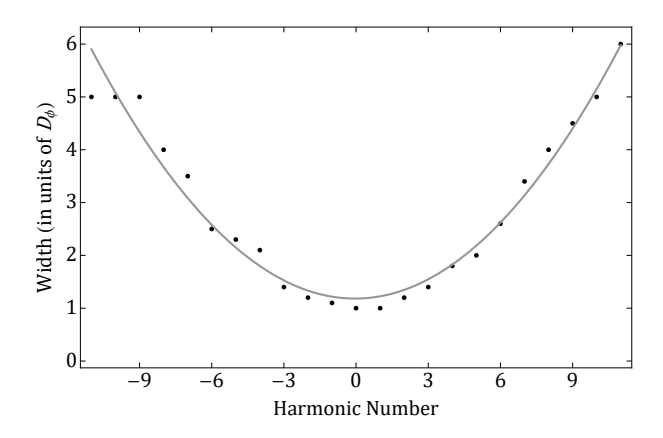


Figure 2: Dependence of linewidth of each tooth on the harmonic number, obtained from the optical spectrum calculated with the LLE under pulsed injection.

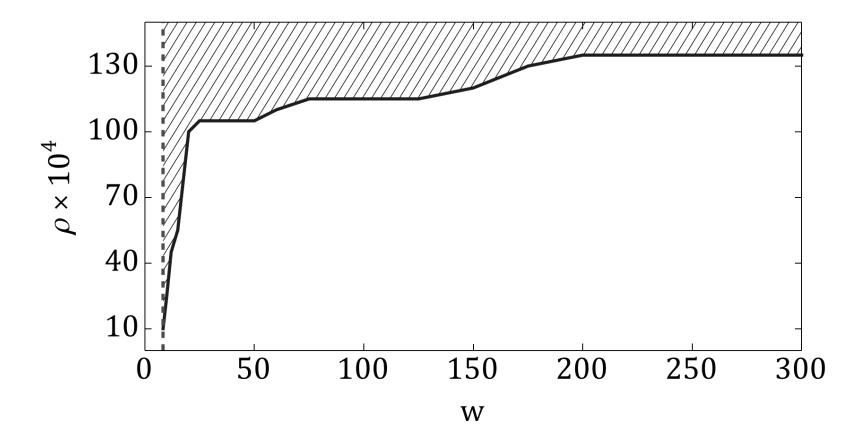


Figure 3: Stable soliton existence as a function of the pulse width w and phase noise amplitude ρ for a fixed detuning under pulsed injection. The dashed line indicates the minimum pulse width w = 8.3; the shaded region marks the noise-induced soliton destruction zone.

4 Noise driven soliton disruption

Increasing the amplitude of the phase noise in the system, described with the LLE and coupled to CW injection, leads to suppression of solitons and a corresponding increase in linewidth. In Fig. 3 the phase noise is defined by Eq. (2) and its amplitude increases from $0.001*10^4$ to $0.0135*10^4$. The region of stable soliton existence shrinks, and above a certain level, the soliton is completely suppressed. A similar effect is observed in the system described by the LLE with pulsed injection. Combined with a sufficiently large increase in pulse width, increase in phase noise amplitude leads to the destruction of the soliton.

We studied the behavior of the region of soliton existence in the case of uniform pump amplitude and constant detuning θ to determine the nature of this effect (Fig. 4 and Fig. 5). The model was analyzed in the presence of phase noise, defined as follows:

$$\phi(t) = \epsilon W_{\phi}$$

The evolution of the real parts of the eigenvalues, which are responsible for soliton destabilization in the noiseless case, is shown in Fig. 4 (b)-(c). θ_{sn} correspond to a value where saddle-node bifurcation

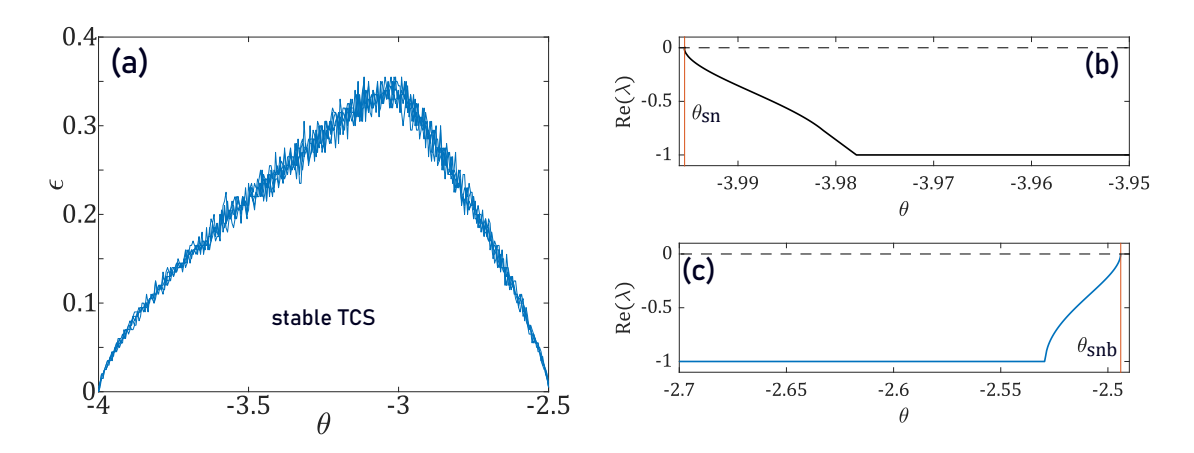


Figure 4: (Color online) Region of the existence of temporal cavity solitons (TCS) in $\theta-\epsilon$ plane with the fixed $\eta_\phi=1.8$ (a). The motion of the real parts of the eigenvalues responsible for TCS destabilization in the noiseless case (b-c).

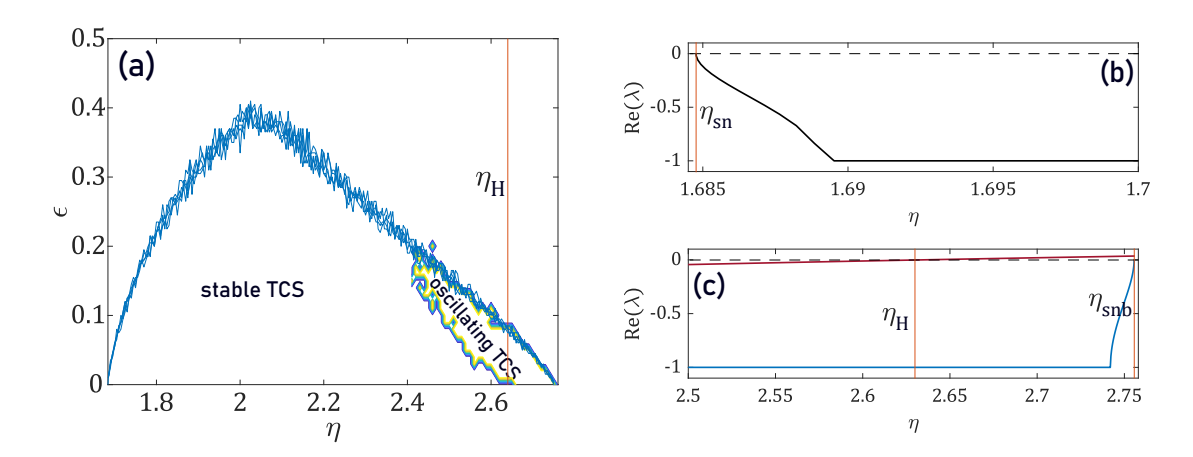


Figure 5: (Color online) Region of the existence of solitons in $\eta_{\phi} - \epsilon$ plane with the fixed $\theta = -3.5$, where η_H line marks the pump amplitude at which soliton undergoes Hopf bifurcation in the noiseless case (a). The motion of the real parts of the eigenvalues responsible for TCS destabilization in the noiseless case (b-c).

of soliton takes place and θ_{snb} corresponds to a value where saddle-node bifurcation of a soliton background (of corresponding CW state) takes place. In Fig. 5 (b)-(c), the values at which the saddle-node bifurcations of the soliton (and the soliton background) occur correspond to η_{sn} and η_{snb} , respectively.

We further analyzed the temporal dynamics and corresponding spectrum of an oscillation soliton following a Hopf bifurcation (Fig. 6(a)). The soliton begins to oscillate in time, which is further confirmed by its spectrum, exhibiting the characteristic limit cycle behavior associated with a Hopf bifurcation.

5 Effect of the optical feedback

In the previous section, we demonstrated that increasing the noise amplitude leads to the destruction of the soliton, which in turn disrupts the output frequency comb, as shown in Fig. 7(a). Phase noise causes the comb to vanish, resulting in an optical spectrum with a single frequency component. How-

50

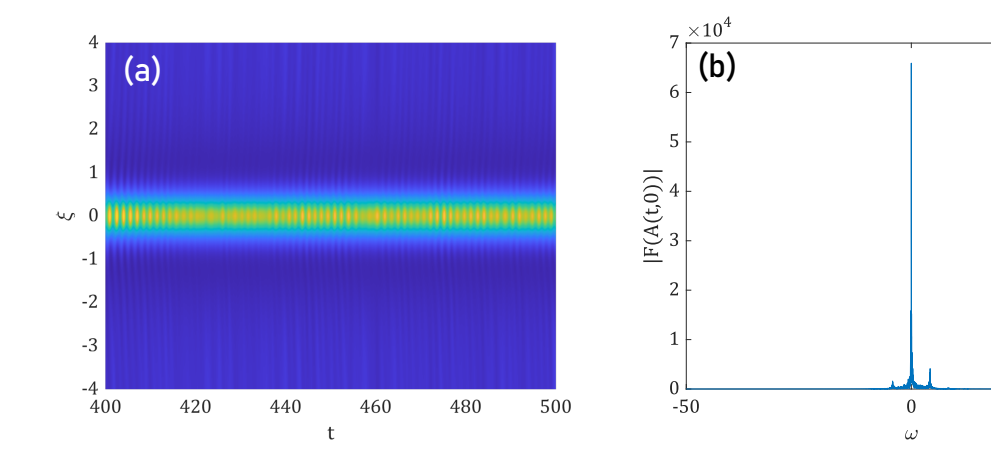


Figure 6: Time dynamics of an oscillating soliton after Hopf bifurcation induced by noise (a). The corresponding spectrum of soliton peak (F(A(t,0))) is the Fourier transform of soliton peak A(t,0)(b). Parameters: $\eta_{\phi} = 2.5, \, \theta = -3.5, \, \epsilon = 0.12.$

ever, it has been experimentally shown that optical feedback from the microresonator to the laser can restore the frequency comb [25]. In this regime, the linewidth of each comb tooth is reduced compared to the spectrum obtained from simulations without feedback, as illustrated in (here should be a paper). To investigate this effect, we coupled the Lugiato-Lefever equation to conventional semiconductor laser rate equations. The resulting model can be written as follows:

$$\frac{\partial A}{\partial t} + v \frac{\partial A}{\partial x} = -(1+i\theta)A + i|A|^2A + i\alpha \frac{\partial^2 A}{\partial x^2} + F(t), \tag{16}$$

$$\frac{\partial F}{\partial t} = (1 + i\alpha)(N - 1)F + \gamma A[L, t - \tau] + \chi_F(t), \qquad (17)$$

$$\frac{\partial N}{\partial t} = -\gamma_N(N - J + N|F|^2), \qquad (18)$$

$$\frac{\partial N}{\partial t} = -\gamma_N (N - J + N|F|^2),\tag{18}$$

in Eq. (16) F is the laser field envelope, which acts as CW injection term in the LLE, and due to group

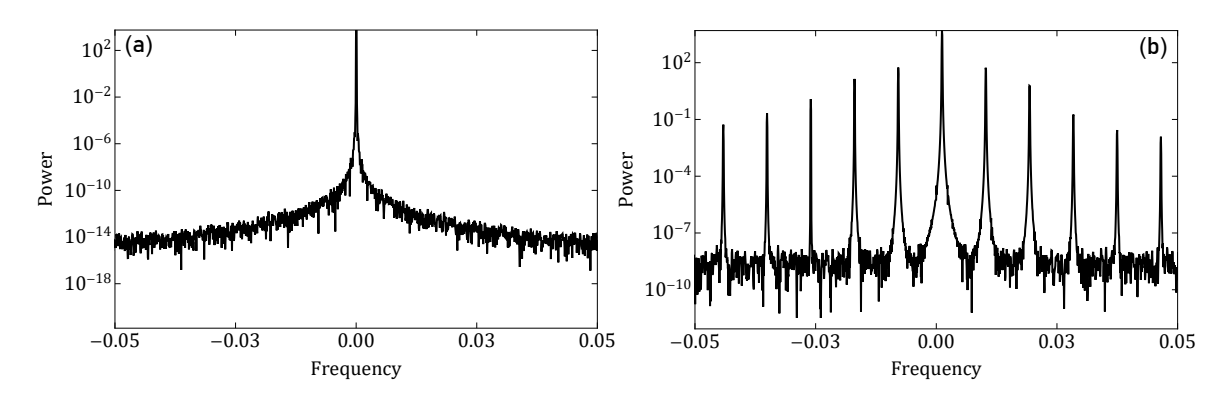


Figure 7: Optical spectrum obtained with Eqs. (16)-(18) with $\gamma=0$ (a) and with $\gamma=0.06$ (b) feedback. Other parameters are fixed at $\theta = \sqrt{3}$, v = 0.1, J = 2.5, $\alpha = 0$ and $\gamma_N = 10$.

velocity term solitons travel within the micro-ring with the speed v. As a result the re-injection term $A[L,t-\tau]$ in Eq. (17) describes a wave-train of pulses with the repetition rate v/L and feedback level γ . N is the carrier density, α is the linewidth enhancement factor, γ_N is the carrier relaxation rate, J is the pumping rate, and χ_F is spontaneous emission noise.

The numerical simulation results are presented in Fig. 7 where the optical spectrum exhibits a single frequency due to phase noise in the absence of feedback, Fig. 7 (a). Figure 7(b) shows the optical spectrum with restored output frequency comb with introduced feedback. Note that the repetition rate v/L is much larger than the laser bandwidth. As a result, the laser predominantly interacts with the cavity mode corresponding to the soliton background, as all the other modes create frequency beating that are filtered out. In this regime, we can adapt the work of Mørk and Tromborg [22] to describe the stochastic dynamics of a semiconductor laser under optical feedback. Their model is based on the Lang–Kobayashi (LK) equations, which govern the evolution of the complex electric field and the carrier density in the laser. In these equations, the envelope of the complex field evolves according to

$$\frac{\partial F}{\partial t} = (1 + i\alpha)(N - 1)F + \gamma F[t - \tau] + \chi_F(t),\tag{19}$$

while the carrier density follows the same form as in Eq. (18). By adiabatically eliminating the intensity and carrier dynamics, we derive a phase equation valid in the weak-feedback regime [15]:

$$\frac{d\phi}{dt} = C \sin\left[\phi(t) - \phi(t - \tau) + \arctan\alpha + \omega_0 \tau\right] + \chi_\phi(t),\tag{20}$$

where $\chi_\phi(t)$ defines the phase noise and $C=\gamma\sqrt{1+\alpha^2}$. After introducing the phase difference $\eta_{LK}=\phi(t)-\phi(t-\tau)$ and using the approximation $\dot{\phi}=\frac{\eta_{LK}}{\tau}+\frac{\eta\dot{L}K}{2}$, Eq. (20) is reduced to:

$$\frac{d\eta_{LK}}{dt} = -\frac{dV}{d\eta_{LK}} + \chi_{\phi}(t),\tag{21}$$

where $V(\eta_{LK})$ represents an effective potential [15]:

$$V(\eta_{LK}) = \eta_{LK}^2 - 2C\cos(\eta_{LK} + \arctan\alpha + \omega_0\tau), \tag{22}$$

Equation (21) can be interpreted as the motion of a particle in a dynamic potential landscape with an associated effective potential [22]. Each well in this landscape corresponds to a phase-locked solution, and noise can induce jumps between these wells, a mechanism known as mode hopping. In [15] the effective potential determines the stability of each external-cavity mode: its local minima correspond to stable operating frequencies, and the curvature at these minima defines how strongly the phase is confined. A deeper potential well limits the amplitude of phase fluctuations driven by spontaneous-emission noise, reducing phase diffusion and leading to a narrower optical linewidth. As already stated, in the model described by Eqs. (16)-(18), the repetition rate of the microresonator pulses exceeds the modulation bandwidth of the laser; consequently, the laser is sensitive only to feedback from the cavity mode associated with the soliton background. The amplitude of this mode can be approximated by analyzing the CW solutions of the LLE as a function of the input intensity, as shown in Fig. (8). The figure illustrates the characteristic bistable response of the LLE, where the lower branch corresponds to the background field on which the soliton is superimposed. The linearisation of the lower branch near the zero-intensity input allows one to establish a linear relation between the input and output intensities, and therefore to estimate the feedback level $\gamma = |A|^2/|F|^2$, which enables the reduction of Eq. (17) to the Lang-Kobayashi equation (Eq. (19) and estimate the linewidth of the laser and frequency comb. This reduction has two main implications. First, it separates the slow dynamics of the laser from the fast intracavity field, allowing the feedback-induced phase evolution of the laser to be analyzed independently of the soliton dynamics. Second, it provides a link between the feedback parameters and the linewidth of the laser and the frequency comb. This relationship clarifies the improvement of coherence in the coupled system through the effect of optical feedback on the laser linewidth.

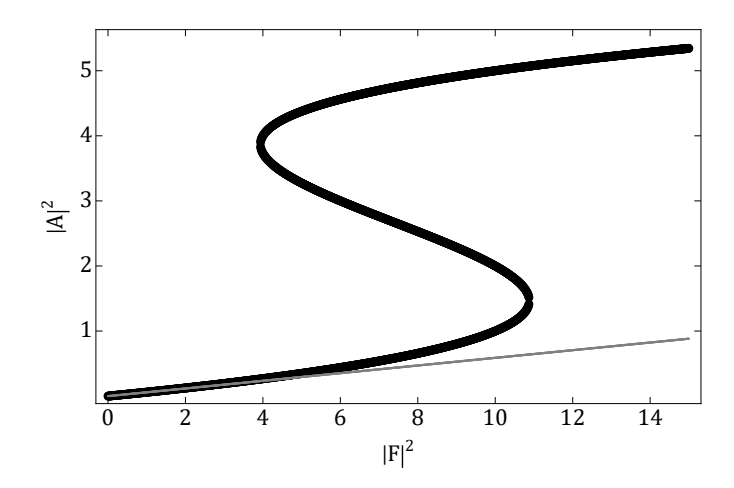


Figure 8: Stationary curve (thick black) and reference line, which is the linear approximation of injection F (thin gray).

6 Conclusion

We have analyzed the coherence properties of Kerr frequency combs generated in optical microresonators under noisy injection and optical feedback, using both analytical and numerical methods within the framework of the LLE. Through asymptotic analysis, we derived explicit expressions for the phase noise and timing jitter, demonstrating that the pump phase noise is directly transferred to the soliton phase, while the timing jitter is strongly suppressed by the restoring dynamics of the intracavity field. The resulting Orstein—Uhlenbeck-type equations describe the stochastic motion of the soliton and demonstrate that, in the limit of CW injection, the timing jitter arises solely from cavity drift noise.

Numerical simulations of synchronously pumped microcavities confirm these theoretical results, revealing a quadratic dependence of the optical and RF linewidths on the harmonic order, a characteristic signature of timing jitter known from mode-locked lasers. Increasing the amplitude of phase noise destabilizes the soliton, leading to its suppression through Andronov—Hopf or saddle-node bifurcations. These bifurcations define the boundaries of stable soliton operation in the presence of noise.

Finally, by coupling the LLE to semiconductor laser rate equations, we showed that coherent optical feedback can restore soliton stability and narrow the linewidth of individual comb lines. The feedback acts through a phase-locking mechanism similar to that described by the Lang-Kobayashi equations and provides an effective means to control phase noise in microresonator-based frequency combs. This work was supported by the HYBRIDCOMB project, funded by the ANR and the DFG (No. 491234846).

References

- [1] M. H. Anderson, R. Bouchand, J. Liu, W. Weng, E. Obrzud, T. Herr, and T. J. Kippenberg. Photonic chip-based resonant supercontinuum via pulse-driven Kerr microresonator solitons. *Optica*, 8(6): 771–779, 2021.
- [2] V. Brasch, E. Obrzud, S. Lecomte, and T. Herr. Nonlinear filtering of an optical pulse train using dissipative Kerr solitons. *Optica*, 6(11):1386–1393, 2019.
- [3] D. A. Dolinina and A. G. Vladimirov. Synchronization between kerr cavity solitons and broad laser pulse injection. volume 11, page 1050. MDPI, 2024.
- [4] D. A. Dolinina, G. Huyet, D. Turaev, and A. G. Vladimirov. Desynchronization of temporal solitons in kerr cavities with pulsed injection. *Optics Letters*, 49(14):4050–4053, 2024.
- [5] M. Erkintalo, S. G. Murdoch, and S. Coen. Phase and intensity control of dissipative Kerr cavity solitons. *Journal of the Royal Society of New Zealand*, 52(2):149–167, 2022.
- [6] M. Erkintalo et al. Coherence properties of Kerr frequency combs. *Optics Express*, 20(24): 27756–27763, 2012.
- [7] Y. Geng, X. Han, X. Zhang, Y. Xiao, S. Qian, Q. Bai, Y. Fan, G. Deng, Q. Zhou, K. Qiu, et al. Phase noise of Kerr soliton dual microcombs. *Optics Letters*, 47(18):4838–4841, 2022.
- [8] T. Habruseva, S. O'Donoghue, N. Rebrova, F. Kéfélian, S. P. Hegarty, and G. Huyet. Optical linewidth of a passively mode-locked semiconductor laser. *Opt. Lett.*, 34(21):3307—3309, Nov 2009. doi: 10.1364/OL.34.003307. URL https://opg.optica.org/ol/abstract.cfm?URI=ol-34-21-3307.
- [9] I. Hendry. *Novel dynamics of driven nonlinear resonators*. PhD thesis, ResearchSpace@ Auckland, 2020.
- [10] I. Hendry, W. Chen, Y. Wang, B. Garbin, J. Javaloyes, G.-L. Oppo, S. Coen, S. G. Murdoch, and M. Erkintalo. Spontaneous symmetry breaking and trapping of temporal Kerr cavity solitons by pulsed or amplitude-modulated driving fields. *Physical Review A*, 97(5):053834, 2018.
- [11] I. Hendry, B. Garbin, S. G. Murdoch, S. Coen, and M. Erkintalo. Impact of desynchronization and drift on soliton-based Kerr frequency combs in the presence of pulsed driving fields. *Physical Review A*, 100(2):023829, 2019.
- [12] T. Herr, J. B. Jensen, T. J. Kippenberg, R. Holzwarth, and S. A. Diddams. Universal formation dynamics and noise characteristics of Kerr-frequency combs in microresonators. *Nature Photonics*, 6(11):946–953, 2012. doi: 10.1038/nphoton.2012.127. URL https://www.epfl.ch/labs/k-lab/wp-content/uploads/2018/09/nphoton.2012.127.pdf.
- [13] N. Kuse and K. Minoshima. Amplification and phase noise transfer of a Kerr microresonator soliton comb for low phase noise thz generation with a high signal-to-noise ratio. *Optics Express*, 30(1):318–325, 2021.
- [14] F. Lei, Z. Ye, Ö. B. Helgason, A. Fülöp, M. Girardi, and V. Torres-Company. Optical linewidth of soliton microcombs. *Nature Communications*, 13(1):3161, 2022.

- [15] D. Lenstra. Statistical theory of the multistable external-feedback laser. *Optics Communications*, 81(3):209-214, 1991. ISSN 0030-4018. doi: https://doi.org/10.1016/0030-4018(91) 90640-Y. URL https://www.sciencedirect.com/science/article/pii/003040189190640Y.
- [16] F. Leo, S. Coen, P. Kockaert, S.-P. Gorza, P. Emplit, and M. Haelterman. Temporal cavity solitons in one-dimensional Kerr media as bits in an all-optical buffer. *Nature Photonics*, 4(7):471–476, 2010.
- [17] L. A. Lugiato and R. Lefever. Spatial dissipative structures in passive optical systems. *Physical Review Letters*, 58(21):2209–2211, 1987.
- [18] A. Matsko, A. Savchenkov, W. Liang, V. Ilchenko, D. Seidel, and L. Maleki. Mode-locked Kerr frequency combs. *Optics letters*, 36(15):2845–2847, 2011.
- [19] A. B. Matsko and L. Maleki. On timing jitter of mode locked Kerr frequency combs. *Optics express*, 21(23):28862–28876, 2013.
- [20] A. B. Matsko and L. Maleki. Conversion of amplitude and phase noise from the pump laser to the repetition rate of a Kerr frequency comb. *Optics Letters*, 40(24):5775–5778, 2015. doi: 10.1364/OL.40.005775. URL https://arxiv.org/abs/1410.8600.
- [21] G. Moille, P. Shandilya, J. Stone, C. Menyuk, and K. Srinivasan. All-optical noise quenching of an integrated frequency comb. *arXiv* preprint *arXiv*:2405.01238, 2024.
- [22] J. Mork and B. Tromborg. The mechanism of mode selection for an external cavity laser. *IEEE Photonics Technology Letters*, 2(1):21–23, 1990. doi: 10.1109/68.47029.
- [23] K. Nishimoto, K. Minoshima, T. Yasui, and N. Kuse. Investigation of the phase noise of a microresonator soliton comb. *Optics Express*, 28(13):19295–19303, 2020.
- [24] F. R. Talenti, Y. Sun, P. Parra-Rivas, T. Hansson, and S. Wabnitz. Control and stabilization of Kerr cavity solitons and breathers driven by chirped optical pulses. *Optics Communications*, 546: 129773, 2023.
- [25] A. S. Voloshin, N. M. Kondratiev, G. V. Lihachev, J. Liu, V. E. Lobanov, N. Y. Dmitriev, W. Weng, T. J. Kippenberg, and I. A. Bilenko. Dynamics of soliton self-injection locking in optical microresonators. *Nature Communications*, 12(1):235, 2021.
- [26] T. Wildi, A. Ulanov, N. Englebert, T. Voumard, and T. Herr. Sideband injection locking in microres-onator frequency combs. *APL Photonics*, 8(12), 2023.